Development of a 2-DoFs actuated wrist for enhancing the dexterity of myoelectric hands

Development of a 2-DoFs Actuated Wrist for Enhancing the Dexterity of Myoelectric Hands

Article *in* IEEE Transactions on Medical Robotics and Bionics · January 2023

DOI: 10.1109/TMRB.2023.3336993

10 authors, including:

Nicolò Boccardo
Istituto Italiano di Tecnologia
35 PUBLICATIONS **338** CITATIONS
SEE PROFILE

Michele Canepa
Istituto Italiano di Tecnologia
24 PUBLICATIONS **300** CITATIONS
SEE PROFILE

Lorenzo Lombardi
Istituto Italiano di Tecnologia
8 PUBLICATIONS **196** CITATIONS
SEE PROFILE

A. Marinelli
Istituto Italiano di Tecnologia
19 PUBLICATIONS **103** CITATIONS
SEE PROFILE

Development of a 2-DoFs actuated wrist for enhancing the dexterity of myoelectric hands

N. Boccardo* *Member IEEE*, M. Canepa* *Member IEEE*, S. Stedman, L. Lombardi, A. Marinelli *Member IEEE*, D. Di Domenico *Member IEEE*, R. Galviati, E. Gruppioni *Member IEEE*, L. De Michieli *Member IEEE* and M. Laffranchi *Member IEEE*

***Abstract*— Developing a prosthetic system that emulates the complexity of the human upper limb is a formidable challenge. Unfortunately, abandonment rates for such devices remain high, primarily due to the limited intuitiveness of control and poor dexterity. Specifically, inadequate wrist mobility, i.e., the absence of actively controllable flexion-extension and pronation-supination degrees of freedom, often results in subpar dexterity in upper limb prostheses. This work introduces an anthropomorphic wrist prosthesis featuring active flexion-extension and pronation-supination capabilities, integrated with the poly-articulated Hannes hand. The central focus of this study is to compare the functionality of this prosthetic system with the natural wrist movement of healthy participants, demonstrating that the biomechanical range of motion falls within that of the mechatronic system. The overarching goal is to improve the performance of trans-radial prostheses by enhancing their dexterity and overall functionality. Our preliminary findings from healthy subjects demonstrate that the incorporation of a 2 Degrees-of-Freedom active biomimetic wrist into the prosthesis can approximate human-like capabilities in upper limb prostheses. Moreover, the resulting development confirm its enhanced dexterity when operated by amputees. These results provide valuable insights into the potential applications of this technology for amputees, offering a basis for future investigations.**

***Index Terms*—Prosthetics, Bionics, Rehabilitation Robotics, Mechatronics, Bioengineering**

I. Introduction

THE human hand is widely regarded as the most intricate and functional part of the human anatomy [1, 2]. Therefore, the loss of an upper limb is a profoundly traumatic event, and engineering a suitable replacement remains a challenge, both from mechanical and control perspectives. As a result of these challenges, long-term abandonment rates of prosthetic devices remain high, ranging from 30-50% [3, 4].

In cases of forearm-level amputation, the loss of the hand is often accompanied by the loss of the wrist joint. The human wrist joint provides two Degrees-of-Freedom (DoFs), the ulnar-radial deviation (URD), and the flexion-extension (FE). However, the pronation-supination (PS) is also lost with forearm-level amputation, despite its anatomical location can be associated to the elbow joint. The loss of these three DoFs significantly affects the quality of life for amputees, as they are essential for manipulation and interaction. It is well-documented, through wrist splinting studies, that the inability to correctly position the hand can hinder even the most advanced prosthetic hands from performing prehensile tasks [5, 6].

As a consequence, the absence of wrist mobility significantly limits the hand's orientation capabilities, forcing compensatory movements [7] that add stress to the body and cause overuse complications in the remaining joints [5, 8]. Bertels [9] demonstrated that even a single DoF prosthetic wrist, coupled with a prosthetic hand, can greatly reduce the amplitude of compensatory movements. Given the importance of wrist mobility to users, it is essential to replicate the functionality of the native human wrist in prosthetic devices, both in terms of available DoFs and control capability [10]. In user-needs assessments, individuals have emphasized the necessity of various improvements, such as multiple passive [11] or active wrist movements, simultaneous control of wrist and grasps, wrist position feedback, among others, for Activities of Daily Living (ADLs) [10].

Nonetheless, user-controllable actuated prosthetic wrists have largely been ignored in the literature, in comparison to the efforts devoted to hand prosthesis development [5, 12, 13]. In fact, there are very few commercial myoelectric wrist prostheses available on the market, chiefly the Ottobock pronation-supination Electric Wrist Rotator [14], the Fillauer MC Wrist Rotator [15] and Fillauer Powered Flexion Wrist [16], all of them offering only one active DoF. In addition, research devices such as the Keshen KS-Bionic Hand with an actuated pronation-supination and flexion-extension wrist [17], the modular and compliant wrist module developed by [18], the ToMPAW modular arm [19] and DARPA Modular Prosthetic Limb [20] DEKA “Luke” Arm [21] have been developed, but have yet to be made commercially available for a prosthetic use [22].

This paper presents an innovative 2-DoFs prosthetic wrist and its development, control, and evaluation, with a focus on its design and ability to replicate ADLs according to user needs. Moreover, we demonstrate how combining this device with the CE-marked underactuated prosthetic hand Hannes [23] addresses the most demanding tasks which other devices fail to accomplish. As consequence, to satisfy users' needs assessment [10], we aim to control this innovative wrist by using learning strategies such as pattern recognition (PR) [24]. This approach results in improved control, both in terms

Corresponding author: N. Boccardo.

** These authors contributed equally to this manuscript*

N. Boccardo, M. Canepa, S. Stedman, L. Lombardi, A. Marinelli, D. Di Domenico, R. Galviati, L. De Michieli and M. Laffranchi, are with the Istituto Italiano di Tecnologia, Genova, Italy (e-mail: nicolo.boccardo@iit.it, michele.canepa@iit.it, sam.c.stedman@gmail.com, lorenzo18.lombardi@gmail.com; andrea.marinelli@iit.it, dario.didomenico@iit.it, riccardo.galviati@iit.it, lorenzo.demichieli@iit.it, matteo.laffranchi@iit.it).

N. Boccardo and M. Canepa is also with the Open University Affiliated Research Centre at Istituto Italiano di Tecnologia (ARC@IIT), via Morego 30, Genova, Italy.

A. Marinelli is also with Bioengineering Lab, University of Genova, DIBRIS, Genova, Italy.

D. Di Domenico is also with the Department of Electrical, Electronics and Communications, Politecnico di Torino, Torino, Italy.

E. Gruppioni is with the INAIL Prosthetic Centre, Vigorso di Budrio, Bologna, Italy (e-mail: e.gruppioni@inail.it)

of naturalness and intuitiveness, of the multi-DoF prosthetic device. Therefore, we showcase the successful application of advanced PR techniques, as presented in [25], in real-life scenarios for this newly developed system.

To provide a comprehensive overview of the research, we first outline the system requirements in Section II. We then delve into a detailed description of the mechanical, electrical, and control design of the prosthetic systems in Section III. The testing methodology employed to validate the overall design is described in Section IV, followed by the presentation of corresponding experimental results in Section V. Finally, in Sections VI and VII, we discuss the potential impact of this work and suggest future applications of the system.

II. System Requirements

The Hannes hand was designed using a bio-inspired holistic approach. The result was an under-actuated hand prosthesis that nonetheless exhibits biomimetic behaviour of the human hand [26]. Hannes is already capable of performing three main categories of grasp, using a passive, manually operated thumb adduction: power grasp, precision grasp and lateral grasp. The under-actuated differential mechanism of the Hannes hand has been already presented and discussed [26], therefore, we focus here on the novel design of the 2 DoFs wrist.

With a similar design approach, our goal was to develop a 2-DoFs prosthetic wrist including flexion-extension (FE) and pronation-supination (PS) characterized by biomimetic performances in terms of range of motions (RoMs), speed and torque hence consenting user to perform the most demanding ADLs.

In the following part of this manuscript, we firstly present the biological and technical requirement as inspired by ADLs (Section II.A and II.B respectively), followed by the kinematic layout (Section II.C) and finally the power and safety aspects (Section II.C and II.D respectively) considered along with the development phases.

A. User's needs-driven requirements

The human wrist joint has three DoFs that can be simultaneously moved. The wrist itself possesses two DoFs: FE and URD. In addition, the forearm ulnar and radius bones provide PS movement [27-29]. Since this rotation ability is largely lost by trans-radial amputees it can be considered integral to wrist functionality and a relevant characteristic for a prosthetic wrist system to fulfil. To be able to effectively replicate the functionalities of its biological counterpart, the hand-wrist prosthetic system should possess the following features [23, 30-33]:

1) RoMs, torques and speed must be comparable to the ones attained by humans during ADLs;
2) Robustness – each actuator must resist peak loading forces substantially above peak torques exerted during ADLs, in case of a fall or improper use;
3) Anthropomorphism – the system must approximate the size of the human hand and forearm;
   a. Low weight – as this characteristic is strongly correlated with abandonment rates, the system must weigh less than the human hand and arm, needing to be similar to commercial prostheses (see Table I) [34];
   b. Low overall length – The type of arm amputation and lost functionality is unique for each patient. The minimum overall length will maximise the number of patients that can benefit from a wrist prosthesis system. As up to 70% of upper limb amputations are distal to the elbow, and assuming that the average trans-radial amputation occurs halfway along the forearm, then the total length of the wrist prosthesis should not exceed 50% of the female 5th percentile of forearm length (around 97mm) [2].
4) Ease of Control and low latency – From the Assessment of user needs [10], it emerges how the wrist is explicitly required by the amputees, since, as already stated, the positioning of the hand is crucial in everyday activities. Moreover, focusing on the users' requirements, the ease of control and the non-disturbing time delay in wrist movements are both crucial. To deal with these, we developed a low-level control strategy (Section III.C) for the wrist and tested the device involving an online control through PR.

B. Design Requirements from the perspective of ADLs

Literature on RoMs, torques and speeds characterizing each joint of the human arm during 23 ADLs and the SHAP test was used to define the desired DoFs, kinematic layout, and desired peak torque and peak joint velocity of each wrist [35]. The SHAP test is a standardized clinical protocol for estimating and comparing patient hand and wrist dexterity in ADLs [36]. Although simulated activities only approximate functional ones [37] they can estimate the minimum required prosthesis performance.

In addition, whilst RoMs during ADLs are well defined by studies of wrist motion, with the worst-case values found in literature used for each joint [38], there is much fewer data and much higher variation regarding joint speeds and torques [12]. Commercial PS wrist devices angular velocity span from 80 deg/s to 180 deg/s [14, 15]. Previously published researches on wrist PS and FE speeds have noted that 175deg/s is a suitable value to be functional [39], whereas for FE prosthesis the target rotation speed is 150deg/s [40]. Information on nominal and peak wrist torques is even more lacking as most studies focus on maximal wrist torques, nevertheless, minimum torque requirements for the FE and PS wrist can be estimated from the literature [41]. However, in Section IV, it was decided to estimate more accurate values from able-bodied volunteers using motion capture hardware.

C. Kinematic Layout Required for ADLs

F. Montagnani et al. demonstrated that the exclusion of the ulnar-radial deviation DoF using a custom-designed orthosis resulted in the smallest increase of compensatory movements

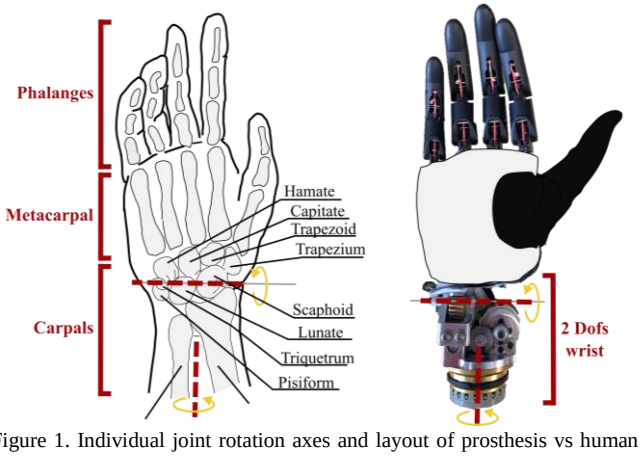

Figure 1. Individual joint rotation axes and layout of prosthesis vs human hand and forearm. 4 mm of misalignment among the human and the wrist.

during the SHAP test [42]. Other studies conducted on able-bodied subjects similarly demonstrated how the URD can be regarded as the least important upper limb movement [43, 44]. In fact, a 2-DoF wrist (PS and FE) coupled with a 1-DoF hand (open/close), performed very similarly to an anatomical hand during SHAP tests.

Based on these findings and the limiting requirement to minimize the prosthetic wrist weight and overall length, a 2-DoFs device with FE and PS was developed, as this would offer similar functionalities compared to a 3-DoFs wrist prosthesis. Moreover, to increase the human-like behaviour, we decided to couple the 2-DoFs wrist with an underactuated prosthetic hand (Hannes) capable to express very high biomimetic performance as demonstrated in [45].

D. Power Consumption Requirements

As an upper limb prosthesis must embed the power source, another important constraint is to minimize the motors power consumption, to gain a sufficient battery autonomy during daily use. As stated in [46], and confirmed during the clinical evaluation performed in 2017 with Hannes [47], transradial amputees perform an average of 150000 main grasp movements per year, resulting in 411 movements per day.

Therefore, we set the requirement to execute at least 500 combined hand and wrist movements with a single battery charge, considering a worst-case scenario of 1:1 ratio between hand and wrist. As consequence, we designed the wrist FE drivetrain to be non-backdrivable, allowing static loads to be resisted without motor torque contribution, therefore greatly minimizing current consumption in static poses [12]. Non-backdrivable transmissions also permit to select smaller motors, since the dynamic active torque requirements during ADLs are low compared to the maximum passive torques that the human wrist can be subjected to [48]. Additionally, the joint will remain static when subjected to sudden external load changes or during a power loss, also resulting in a more predictable control and safer use by upper-limb prosthetic users.

III. Design

In this Section, the prosthetic system will be analyzed in all its parts. Firstly, in Sections 0 and III.B, respectively the mechanical and electrical architectures of the device will be described in their entirety. Subsequently, in Sections III.C and III.D, the control strategies, both low and mid-level, applied to this system will be discussed and detailed.

A. Mechanical Architecture

The mechanical structure of the wrist is intentionally designed to be both serial and modular (Figure 1). This is achieved by creating separate FE and PS wrist joints (Figure 2 and Figure 3, respectively), which can accommodate an Ottobock compatible quick-disconnect Locking Unit [49] and an electrical slip-ring, known as the Coaxial Plug [50] with its corresponding Co-Axial Bushing [51], within the wrist socket. The slip-ring provides power and control signals to the hand during PS rotation. Furthermore, the modular design architecture allows for a flexible overall system length, ensuring the adaptability of the prosthesis to the patient's amputation type and severity (whether distal or proximal), while also preserving compatibility with existing amputee socket. This precluded the investigation of an integrated parallel wrist mechanism for simultaneous multiple DoFs motion such as Stewart-platforms or quaternion wrists, even though such systems are often more compact than serial chain devices [52].

TABLE I
Biological & ADL Requirements

Joint	Length [mm]	Mass [g]	ADL RoM [deg]	Peak Torque [Nm]	Velocity [rad/s]
Wrist FE	20-30	100	-70 to 50	-3.5 to 3.5	4
Wrist PS	60	100	-65 to 77	-6.0 to 4.0	7
Wrist URD	50	150	-18 to 20	-0.2 to 0.3	-0.2 to 0.3

1) FE Wrist Design

According to the previously presented design requirements (section II), hereafter we describe the design solution to match the anthropomorphism of the FE wrist rotation axis equipped on the Hannes hand. The misalignment between the mechanical and the anatomical rotation axis has been designed to not exceed 5 to 7mm (Figure 1). Moreover, the overall mechanism needed to be as small and noiseless as possible to prevent user discomfort [53]. On the other hand, non-backdrivability was selected as a crucial feature to prevent excessive battery consumption in case of high static loads. Therefore, the FE wrist has a weight of 211g, and its powertrain presents a 3-stage gearbox directly connected to the drive motor (Faulhaber BXT22H) and a slow shaft encoder (Figure 2A). In detail, the first stage is a [(13/3):1] planetary gearbox, that allows lowering the revolutions-per-minute (RPMs) of the BLDC motor while keeping high efficiency ($\eta \approx 0.9$) that guarantees high torque to drive the subsequent gear-stage. The second stage shifts the rotation axis to the physiological position of the human wrist with a [2:1] spur gear to reduce angular velocity by still maintaining high efficiency ($\eta \approx 0.9$).

The supplementary reduction of the resultant angular velocity is fundamental to reduce the noise of the previous

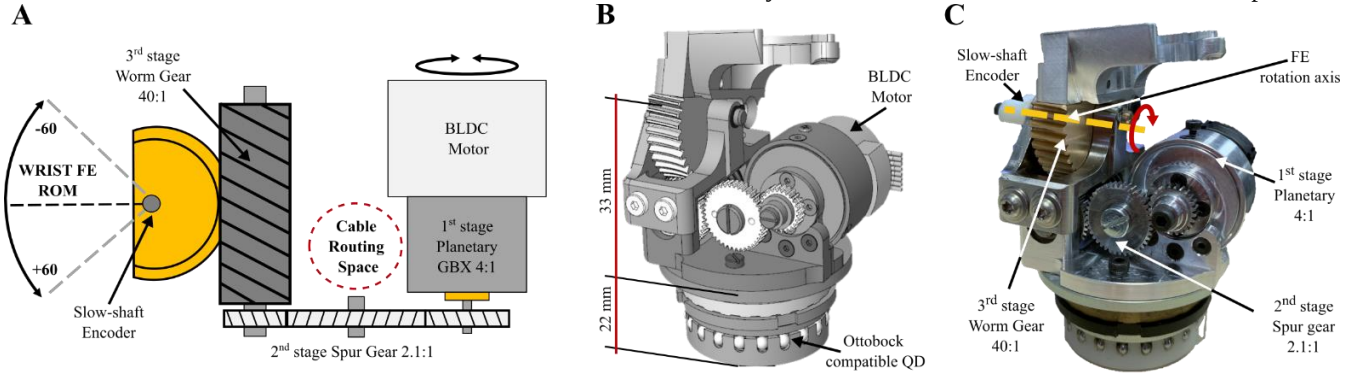

Figure 2. FE wrist: A) Simplified diagram of mechanical design, B) Placement of the mechanical components and C) the real FE wrist device.

gear's stages and to provide a sufficient torque to the third stage although this latter provides low efficiency ($\eta < 0.4$, $0.25 < \eta < 0.4$) [40:1]. Thanks to its precise dimensioning, this third stage (worm-gear) guarantees the correct alignment of the rotation axis. Moreover, it is crucial to grant the non-backdrivability of the entire mechanism, by means of its low efficiency. This characteristic, coupled with the correct dimensioning of the frame, makes the wrist able to hold up to 50 kg in steady condition without any battery consumption. Therefore, the user can lean on the wrist, for example, when standing up from a chair leveraging on the upper limb for stability purposes and reducing harmful compensatory movements.

The design of the entire wrist FE mechanism permits 82 deg of RoM by offering 33 deg in extension and 49 deg in flexion therefore mimicking the natural conditions (40 deg in extension and 38 deg in flexion hence admitting and 78 deg of overall RoM) of healthy subjects [44]. Finally, the resultant mechanism is characterized by an overall length of 55 mm and a 45 mm diameter (Figure 2B).

2) PS Wrist Design

The PS wrist main design requirement was to be hollow shafted, to allow fitting the single slip-ring located in the Ottobock-style Laminating Ring [54]. The weight of this component is 210g and its actuator unit is composed by a frameless PMSM motor (TQ Motors ILM-25x04) [55], directly integrated with the strain-wave reducer's wave generator [100:1] (Harmonic Drive HFUC 11-100-2A R), forming a hollow shaft actuator for electrical connecting the hand prosthesis with the socket electronics. The output of the strain-wave reducer is connected to the female output of the quick-disconnect adapter. The design permits the hand prosthesis and FE wrist actuator to be quickly attached and detached by the patient, whilst ensuring a robust electrical connection between the two halves of the prosthesis system, namely the hand and the socket.

The resultant mechanism is characterized by an overall length of 65.1 mm and a 43 mm diameter (Figure 3C) which offers a one-to-one replacement with the Standard wrist quick-disconnect male (Ottobock-like Locking Unit) and its related counterpart, the Ottobock-like Laminating Ring [56] which can also accommodate the active component namely Electric Wrist Rotator [57] by Ottobock.

On the mechatronic side, our custom device can exert higher angular velocity and torque on the slow shaft in respect to existing commercial solutions (pick torque of around 6 Nm and maximum angular velocity around 70 rpm). The direct connection between the Harmonic Drive and the BLDC motor [55] grants a single reduction stage (Figure 3). The overall power-train efficiency of 80% can be achieved by aligning the bell-shaped efficiency behaviour of the reducer with the one described in the motor datasheet. Conversely, commercial prosthetic wrists offer a cascade of reduction stages that lower the device's efficiency. As consequence, our solution aims at increasing the overall efficiency to design a reversible mechanism that, at the same time, allows the Ottobock-like Locking Unit to disconnect the wrist from the hand thanks to the breakaway torque of the powertrain.

B. Electrical Architecture

From the electrical point of view, the entire system guarantees all the necessary safety features as for IEC60601-1 medical device standard, including sensor diagnostics, overcurrent, overload and short circuit protection as well as compliancy of EMC standards on all the active joints. Moreover, the system is conceived to be modular and self-contained (Figure 4): the hand itself contains all the motor drive electronics necessary to move the main grasp motor and the FE wrist motor in closed loop. All the hand and wrist movements are controlled via a single microcontroller (Texas Instruments TM4C123GH6PM [58]) embedded in a single rigid-flex control board system (SCMM), minimizing space requirements and power consumption overhead. The onboard electronics include a 9-axis IMU module [59], to provide the angular orientation of the hand expressed in quaternions via I2C protocol to the motor control unit of PS wrist (SCMPS). The system includes two contactless absolute on-axis magnetic encoders (AMS AS5045B [60]), to provide absolute position feedback and diagnostics via SPI protocol. The overall system architecture includes a central processing board (EMGM) and up to 6 surface electromyography (EMG) sensors, compatible with both Ottobock electrode or custom circular EMG sensor Marinelli, et al. [61] developed by Rehab Technologies lab of Italian Institute of Technology. The EMGM board hosts a microcontroller (Texas Instruments TM4C123GH6PM), acquiring the EMG signals. The EMGM board is placed above the wrist joint, and acts as a master of a CAN Bus network, sending position references to the SCMM board, for controlling hand and wrist FE via SCMFE, and retrieving various measurements from the SCMM board, such as the joints current, the measured joint position, the angular orientation, and the system status. Additionally, the EMGM board hosts an IMU module to gain information about the angular orientation of the stump and to

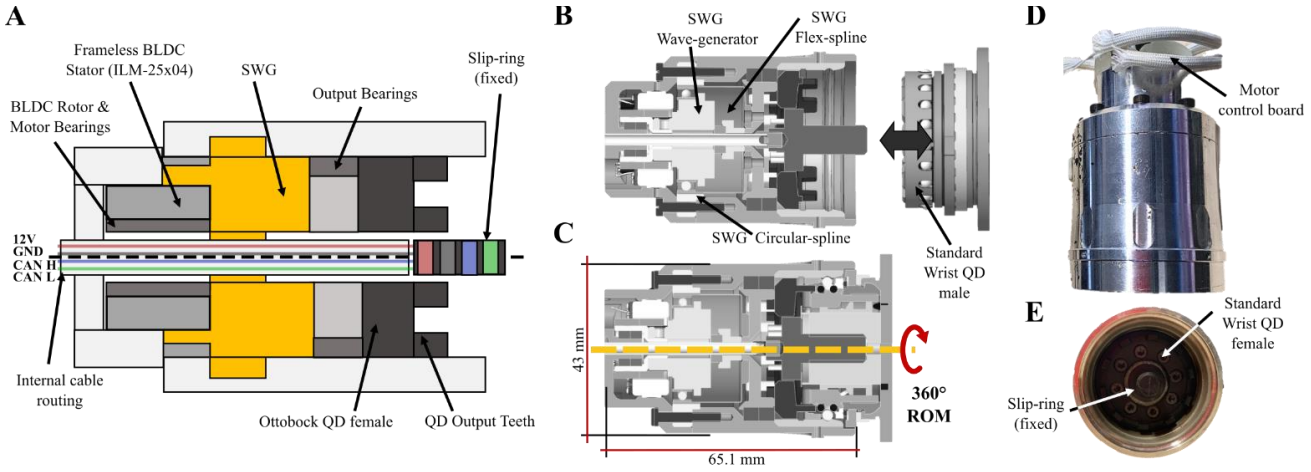

Figure 3. PS wrist: A) Simplified diagram of mechanical design, B) Placement of the mechanical components and C) the real FE wrist device.

TABLE II
Daily power consumption

Joint	Average Current [A]	Average Power [W]	Energy per Movement [J]	Movement Time [s]	Number of Movements	Overall day energy consumption [J]	Percentage on battery charge [%]
Hand	0.75	9.2	7.4	0.8	500	3700	3.7
Wrist PS	0.2	2.4	3.5	1.5	500	1750	1.75
Wrist FE	0.16	2	5	2.5	500	2500	2.5
Idle state	0.07	0.86	-	-	-	48240	48
Total			-			**56209**	**56.2**

directly control the PS wrist control board (SCMPS) movement accordingly (Section III.C).

All the information gathered by the prosthetic systems is then provided via Bluetooth Low Energy to a host system graphical user interface (GUI), which can allow both therapists or researchers to perform tuning of the control parameters, the activation thresholds, check the system diagnostics, visualise, and log the data in real-time. All the data are available to a frequency up to 100Hz via custom communication protocols.

The system is equipped with a custom battery pack, made of 3 lithium-ion certified cells in series (11.1 V nominal, 2.5 Ah capacity, 27.75 Wh energy, 99900 Joule) and a battery management system, carefully designed to fit in the gap between the residual stump and the wrist joint, hence allowing to directly embed the system electronics and power supply in most of the transradial amputation cases. To confirm that, we made a simple evaluation of the power consumption, measuring the battery current absorption at a fixed voltage (12.28 V) in respect of the worst-case movements of each joint (highest speed), using an oscilloscope (Tektronix MDO3034) and a current probe (Tektronix TCP0020). We then computed the net electrical power and the energy absorbed for each task. Additionally, we measured the overall system consumption in an idle state, with all the motors enabled but not moving. With respect to the daily energy balance, we considered a 16 hours per day duty cycle, compared to the energy available with a full charge. The analysis, resumed in Table II, shows that the main energy use is due to the idle state (48%) rather than during the movements. However, is shown that the system can be easily operated, in an average use, for 16 hours consecutively with a single charge, having a good residual charge (43.8%).

C. *Motion Control*

We developed a control strategy that allows both intuitiveness and non-disturbing time delay, in agreement with the assessment of user needs [10]. For the FE wrist joint we implemented a position Proportional-Integral-Derivative (PID) controller by using the custom encoder as feedback (see Figure 2C). Conversely, due to the lack of space, no embedded encoder was possible to fit in the PS joint. Therefore, a virtual encoder was used as feedback to the PS position loop. In particular, the virtual encoder is obtained by using two IMUs (Bosch Sensortech BNO055 [59]) located on the two links, respectively the hand and the socket. These sensors extract quaternions used to compute the angular PS position via a custom algorithm. The "Relative Angle and Orientation" (RAO) algorithm computes the angle between the hand and the forearm, avoiding singularities. To ensure IMUs reliability as a virtual encoder, a two steps calibration is required. The first step is performed once when mounted on the device during which the BNO055 records and stores in the EEPROM offsets for each sensor to compensate for drift and tilt inaccuracies. The second one consists of switching on the device horizontally aligning the z-axes along the gravity direction to ensure long-time stability. The entire procedure is presented hereafter.

Knowing the standard definition of a quaternion ($\boldsymbol{Q}$) and its conjugate ($\boldsymbol{Q}^*$):

$$Q = [q_w, q_x, q_y, q_z] \qquad Q^* = [q_w, -q_x, -q_y, -q_z] \tag{1}$$

setting Q_{pre} and Q_{post} as quaternion relative respectively to pre-joint and post-joint link, it is possible to define the rotation quaternion of the joint as follows:

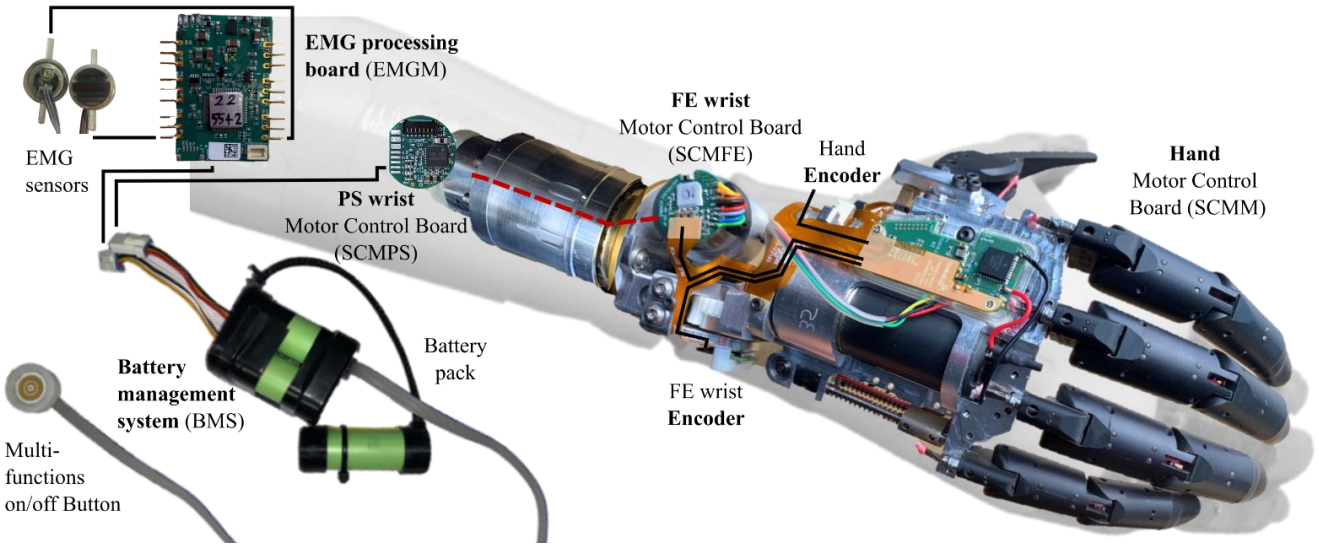

Figure 4. Electronic architecture of the full Prosthetics system.

$$Q_R = \left[Q^*_{pre} \cdot \left(Q_{post} \cdot Q^*_{pre}\right)\right] \cdot Q_{pre} \quad (2)$$

Once Q_R is evaluated by knowing the actual possible DoFs of the joint, the angles along the principal axis (α_x, α_y, α_z) can be computed. Knowing the structure of the quaternion from Eq.(1), the angles can be calculated as follows:

$$\alpha_i = 2 \cdot atan\left(\frac{Q_{R_i}}{Q_{R_w}}\right) \quad \text{, with } i \in [x, y, z] \quad (3)$$

Calculations run in a built-in routine on the EMGM board, retrieving link quaternions from the peripheral sensors and computing the RAO algorithm. This computation efficient routine can run in real-time, as it computes the angles in 0.172 ms (13760 clock cycles) on an ARM Cortex M4F running at 80 MHz.

D. *Pattern Recognition Control*

Furthermore, we implemented a Prosthetic Control (PR) algorithm using Nonlinear-Logistic Regression (NLR) as presented in two our previous works of Marinelli, et al. [25] and Di Domenico, et al. [24]. After training, users controlled 2 and 3 Degrees of Freedom (DoFs) in real-time. The software had two layers: joint selection and joint control. PR decoded user intention using up to 6 EMG electrodes, modulating joint positions based on RMS of EMG signals, with threshold comparison and gain amplification as shown in Figure 6 according to the formula:

$$Joint_{pos} \mathrel{+}= \frac{(RMS(sEMG) - LTh)}{HTh} * Gain \quad (4)$$

where, RMS is the root mean square of the EMG signals, LTh is the activation threshold optimized according to the validation set, HTh is the high threshold EMG coefficient used to normalize the signal amplitude optimized according to the calibration phase and Gain is a parameter to tune the joint speed according to the user needs.

IV. Test Methodology

We developed a 3-phases testing methodology to incrementally characterize and validate the device performances. A preliminary analysis in the frequency domain was performed to identify the dynamic behavior of the single joints' movements as presented in Section IV.A. Subsequently, in Section IV.B we acquired the kinematics of able-body subjects performing ADLs and then used this information to validate the prosthesis' performances in mimicking these movements. Finally, a speed-torque analysis was conducted to outline the mechatronics performances achieved during ADLs as presented in Section IV.C. Moreover, to examine the control capabilities, an EMG-based PR algorithm was developed and tested on amputee as presented in Section IV.D.

A. *Dynamic tests*

We aimed at estimating the bandwidth of the wrist actuation unit in both PS and FE joints. To this end, we imposed a sequence of sinusoidal speed references, by increasing the frequency with step increments of 0.25Hz from 0.25 to 4.5Hz. Moreover, we chose the reference amplitude according to the mechanical RoMs of the system not to impact with the end of travels. We supplied the motor drive with fixed voltage and measured the joint speed output response comparing them with the imposed references. We then interpolated the voltage-speed transfer function to estimate the closed-loop mechanical bandwidth.

B. *Able-Body Kinematics Recording*

To the best of the authors' knowledge, there is a lack of accurate velocity (and torque) profiles of the human wrist joint during typical ADLs in literature. Therefore, we built a dataset of healthy subjects' wrist speed profiles performing multiple tasks. We then obtained reference kinematic trajectories to be applied to the 2-DoF wrist [62] to test its

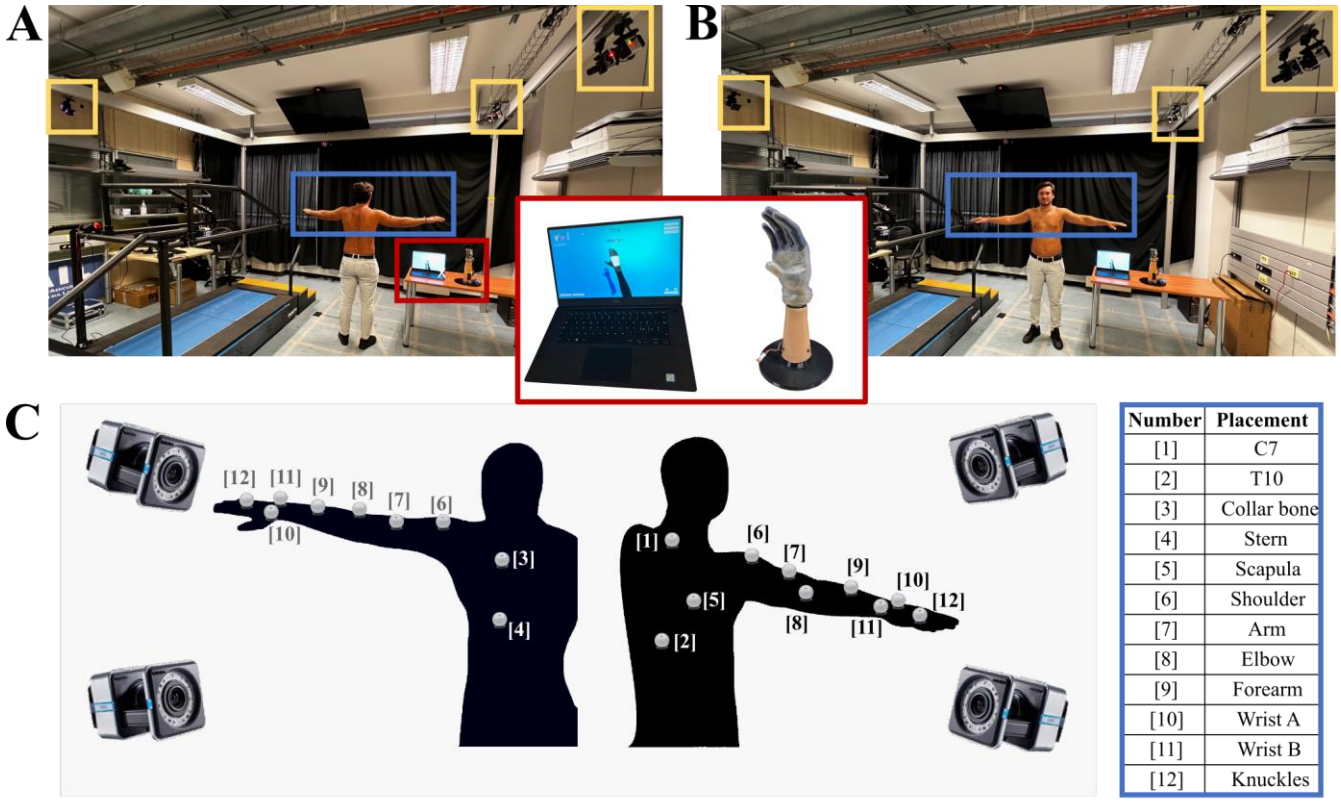

Number	Placement
[1]	C7
[2]	T10
[3]	Collar bone
[4]	Stern
[5]	Scapula
[6]	Shoulder
[7]	Arm
[8]	Elbow
[9]	Forearm
[10]	Wrist A
[11]	Wrist B
[12]	Knuckles

Figure 5. Human-Prosthetic validation setup. A-B) VICON Mo-Cap room, in yellow squares the IR VERO Cameras for marker tracking while in blue square the subject wearing the 12 markers. C) Marker positioning scheme according to VICON user's manual.

dynamic performance under load. The considered tasks were divided into two sections, namely the basic functional tests and fully functional tests. In the former, the subject separately performed simple movements (i.e., wrist flexion, wrist supination) and their combination (i.e., infinite trajectory). In the latter, we selected ADLs activities where the wrist movements play an essential role and recorded the joint angles via a Motion Capture system described below. Eventually, each subject was asked to perform 5 tasks divided as presented in Table III.

In detail, during the trials, the subjects were asked to perform each one of the tasks three times. Using a metronome, a rhythm was prescribed to impose three different speeds, namely "slow" (30bpm), "normal" (45bpm) and "fast" (60bpm). The subjects were asked to perform the task in the most natural way while following these rhythms to start each movement. Moreover, the participants were instructed not to restrict their movements in any way. Imposing a defined time frame to execute the task prevented unnecessary interruptions which could bias the acquired speed distribution. Therefore, a distribution of natural speeds was acquired and compared with the speed performances of the two wrist motors.

As shown in Figure 5, the setup consisted of a Vicon Nexus system, based on 10 Infra-Red (IR) cameras that record the movement of 12 IR-reflecting markers. This system can guarantee a 0.01mm precision over a 48 m^3 of total volume of acquisition. This setup with the 12 IR markers allows the tracking of the whole arm, and, for this case, the detailed movement of wrist PS and FE. The Vicon system has a fixed frame rate of 100Hz. This is consistent to Khusainov et al. [63], as 90% of human movements are under the 5Hz threshold. Therefore, we asked 8 able-bodied volunteers (age range: 25-32 years, 5 males and 3 females with self-reported hand and wrist dominance) to sit on a chair with their elbows fixed and close to their torso to minimize elbow and shoulder contribution. After the participants were marked with the 12 IR markers (according to the marker placement depicted in Figure 5C) they were asked to perform the 9 tasks. During each task, the movement was repeated 10 times. Each subject performed each task with a 30s pause between them to prevent muscular fatigue. The test duration was approximately 20 minutes per participant. The study adhered to the standard of the Declaration of Helsinki and was approved by the Bologna-Imola ethical committees (CP-PPRAS1/1-01).

C. Prosthesis Kinematic and Dynamic Test

We tested the speed and torque performances of the novel prosthetic wrist with the aim of assessing its reliability and its consistency in comparison with the natural equivalent. Therefore, we computed the joints speed Probability Density Function of healthy subjects examined to obtain a reference distribution curve. The percentiles distribution of angular velocities was compared with respect to the speed performances for both PS and FE mechanisms. To this end, we chose the two most demanding basic functional tasks mentioned before for each DoF, executed at maximum achievable rotational speed. To stress the overall system in a realistic scenario, we loaded the prosthetic hand with a glass jug (300 gr) with 500 ml of water for the jug pouring task (PS), and a heavy aluminium sphere (532 gr) for the lifting task (FE). We recorded the joint position and the motor current to compute both speed and torque achieved. From this data we extracted the speed-torque required by the two powertrains while executing the tasks.

TABLE III
Performed tasks

Basic functional	Fully functional
Wrist Flexion-Extension	Stirring
Wrist Pronation-Supination	Jar Pouring
Infinite shape (combo FE and PS)	-

D. Overall system validation

Advanced control strategies [64, 65] were tested on a prosthetic system, initially on healthy subjects and later on amputees. An EMG-based PR algorithm, developed by Di Domenico, et al. [24], enabled simultaneous control of three active DoFs: the Hannes hand's, PS, and FE wrist. The algorithm used speed proportional to EMG signal RMS and achieved simultaneity by activating multiple joint movements. Testing involved 10 healthy subjects and 3 mono-lateral amputees, with each subject performing 10 repetitions of gestures like hand opening and wrist movements. Muscular activity was recorded using 6 MyoBock electrodes (Ottobock) (Figure 6)

. Data collection was managed with EMG-Data Acquisition and Training Software [24]. Non-Linear Logistic Regression [24, 25] was used as the PR algorithm to select the joint to move and map muscle activation to joint reference positions. An example of a subject is reported in Figure 6A, where for each movement and DoF the activation of the six EMGs generate a different pattern associated to the movement intention.

Non-Linear Logistic Regression was used as PR algorithm to select the joint to move, as already offline tested by our group in different configurations. Moreover, we mapped muscle activation amplitude to selected joints' reference position Figure 6C), as described in formula (5):

$$\begin{cases} P_t = P_{t-1} + \Delta S \\ \Delta S = \dfrac{\left\| \sqrt{\frac{1}{N}\sum_{n=1}^{N} |EMG_n|^2} \right\|}{Fc} \end{cases} \quad (5)$$

where P indicates the position, the sum of the previous position and the increment (ΔS). ΔS is calculated with the normalized RMS of the N = 6 EMGs divided by the loop frequency of the microcontroller (300 Hz) to limit the maximum increment to a value that controls the prosthesis full-RoM movement in 1s.

V. RESULTS

Correspondingly with the methods presented in Sec. IV, we computed the open-loop Bode diagram (Section IV.A), the able-body kinematics analysis (Section IV.B) and the joint's speed-torque dynamic performances (Section IV.C). Finally, in Section IV.D we present the results obtained in a real scenario, in which machine learning techniques were used to offer an intuitive control strategy for the multi-DoFs system via EMG.

A. Dynamic test results

This analysis (Figure 7A) shows the speed closed-loop mechanical bandwidth of the prosthetic wrist drive at the maximum battery voltage (12.6 V), defined as the intercept

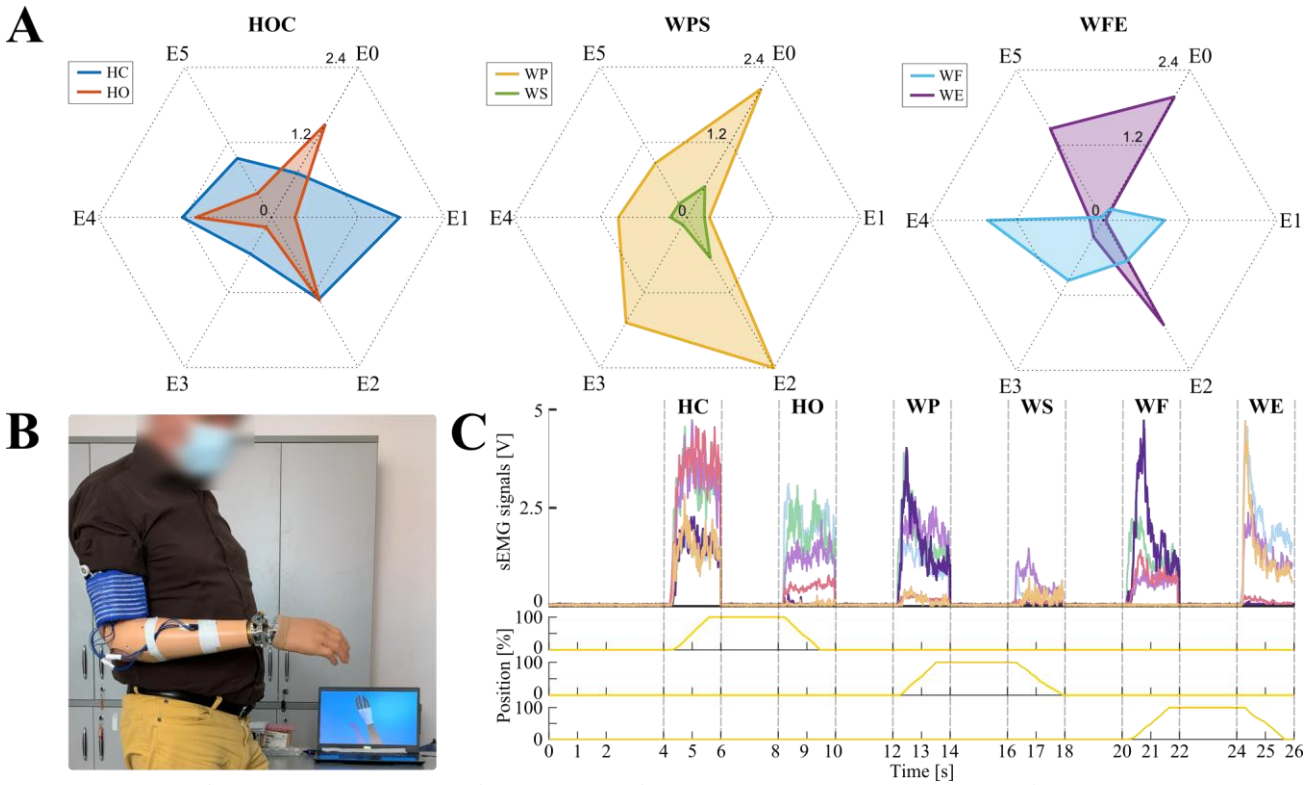

Figure 6. A) Radar plots of the EMG activation separately for the 3 Degrees-of-Freedom: Hand Open and Closure (HOC) (left), Wrist Pronation and Supination (WPS) (center), Wrist Flexion and Extension (WFE) (right). B) Fully integrated, wearable system fitted on a transradial amputee while operating the prosthesis. C) Plot of 6 EMG signals enveloped and amplified (top) compared to the normalized position measurements of the controlled joints (bottom).

of the magnitude system response with the -3dB attenuation red line. The measured dynamic is around 1Hz for wrist PS joint and 2Hz for FE joint in their complete RoMs.

B. Able-Body Kinematic recordings results

Throughout the trials, the participants were instructed to perform movements without any specific guidance, ensuring that the angles measured were not influenced by any bias. Despite this, as depicted in Figure 7B boxplot, the healthy subjects' executed movements were contained within the mechanical Range of Motion (RoM) of the Hannes system. The prosthesis minimum and maximum RoM are indicated by the dotted lines. Specifically, the End-of-Travels for the FE wrist were designed to span from -49 deg to +33 deg, while the Wrist PS could move freely without any restrictions; however, the End-of-Travels were set to span from -90deg to +90 deg. Therefore, these limits could be adjusted according to the subject's natural contralateral anatomy. In the boxplots, the squared regions represent the population from the 25th to the 75th percentile, the grey dashed lines indicate the entire population span and the red crossed indicates the outliers outside the Tukey fence.

C. Performance Characteristics during ADLs

Figure 8A presents the human wrist's speeds distribution compared to the prosthetic wrist speed performance. The Probability Density Function of healthy speeds, as well as the Distribution of the speed population in the form of a boxplot can be appreciated for both PS and FE wrist. These results are compared to the Hannes wrist's performance, represented by the grey shaded area. For the PS joint, we observed a median value of 5.82 rpm (34.95 deg/s), a 25th percentile of 1.51 rpm (9.06 deg/s) a 75th percentile of 16.39 rpm (98.34 deg/s) and a maximum of about 38.7 rpm (232.2 deg/s). For the FE joint, we observed a median value of 4.77 rpm (28.62 deg/s), a 25th percentile of 1.25 rpm (7.5 deg/s) a 75th percentile of 10.12 rpm (60.72 deg/s) and a maximum of about 23.43 rpm (140.58 deg/s). The red crossed indicates the outliers outside the Tukey fence. Moreover, we observed that the data are substantially symmetric with respect to the sense of rotation.

Figure 8A depicts the torque-speed behaviour of the PS and FE wrist respectively performing the two most demanding selected tasks. The maximum rotational speed achieved by PS wrist joint was around 360 deg/s (60 rpm) during glass jug pouring task whilst was around 180 deg/s (30 rpm) for FE wrist while lifting a heavy sphere. The maximum torque exerted by PS wrist joint was around 5.27 N during glass jug pouring task whilst was around 2.38 Nm for FE wrist while lifting a heavy sphere. The dashed grey lines represent the power rating under load and no load, respectively 20 W and 10 W for the PS and 4 W and 2 W for FE wrist. We measured an RMS torque of 1.55 Nm for PS and 0.88 Nm for FE.

D. Control Design Test

Once the NLR classifier was trained, each subject was able to intuitively control the 3 different joints. The implemented control strategy (NLR) was able to suitably discriminate the patterns for the 6 different gestures as presented in Figure 6A. The radar plots show the 6 EMG signals contribution among the classified movements. As consequence, the trained algorithm was able to decode the user intention and translate them into prosthesis actions. In Figure 6C, it is possible to appreciate the synthesis of the position references according to the EMG signals: in the upper side of the graph, EMG rectified signals are grouped together, in the lower side, we show the respective reference positions after the regression. Figure 6B shows the fully integrated system controlled by a transradial amputee. Since the NLR algorithm runs directly embedded in the EMGM control electronics, the system is wearable and usable in a realistic clinical scenario. As a result, the subjects were able to control the prosthesis' RoMs by combining each movement as for ADLs.

VI. Discussion

The aim of this study was to introduce a groundbreaking prosthetic wrist that features 2 degrees of freedom combined with a poly-articulated prosthetic hand. Our primary objective was to evaluate its reliability as a practical substitute for the natural counterpart. To achieve this goal, we conducted a comprehensive multi-level validation process. Our solution, which fully integrates mechanical, electronic, and software components, was designed to meet the requirements outlined in Section II. We developed a compact mechanical assembly, a modular, wearable, and battery-operated electronic structure, and an advanced software system that enables the prosthesis to function in a natural manner.

Initially, we conducted a mechanical bandwidth analysis to explore the frequency response of the two powertrains, showcasing the advanced mechatronics capabilities as presented in Figure 7A. Secondly, we conducted an acquisition campaign on able-bodied individuals to capture wrist movements during typical daily activities, thereby extracting realistic dynamic behaviors. Consequently, we compared the performance of healthy wrists to that of the prosthetic counterpart, evaluating the biomimicry of the proposed mechatronic system in terms of range of motion and speed performance. The suitability of wrist for executing all examined tasks is evident from the RoMs achieved, as depicted in the diagrams of Figure 7B. Furthermore, to assess the wrist's capabilities, we statistically analyzed the speed behavior of natural, healthy wrists and compared the results. From Figure 8A, it is evident that 2-DoFs wrist's speed performance exceeds the maximum statistical angular velocities required for natural tasks, excluding the outliers. This is coherent with the torque-speed performance graphs (Figure 8B), which shows that the worst-case load speed-torque trajectory examined falls inside the limits of the mechatronic system. Human-like dexterity was validated using a ML-based multi-DoFs control strategy on healthy subjects and an amputee (see Supplementary Materials Video). Low control latency and anthropomorphism were crucial for mapping muscular contractions to natural prosthesis movements. The ML approach effectively controlled the system, enabling predictable wrist movements

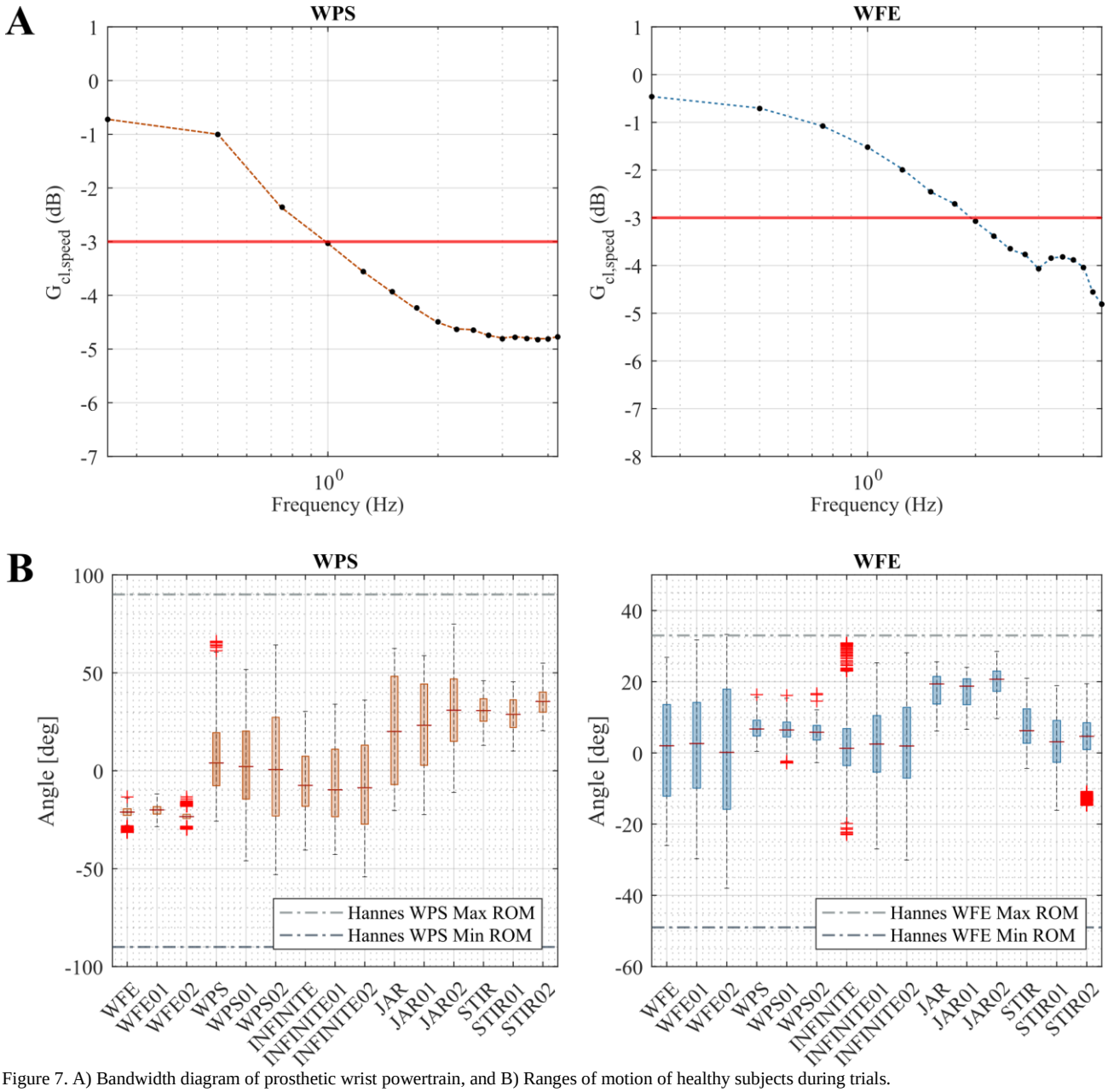

Figure 7. A) Bandwidth diagram of prosthetic wrist powertrain, and B) Ranges of motion of healthy subjects during trials.

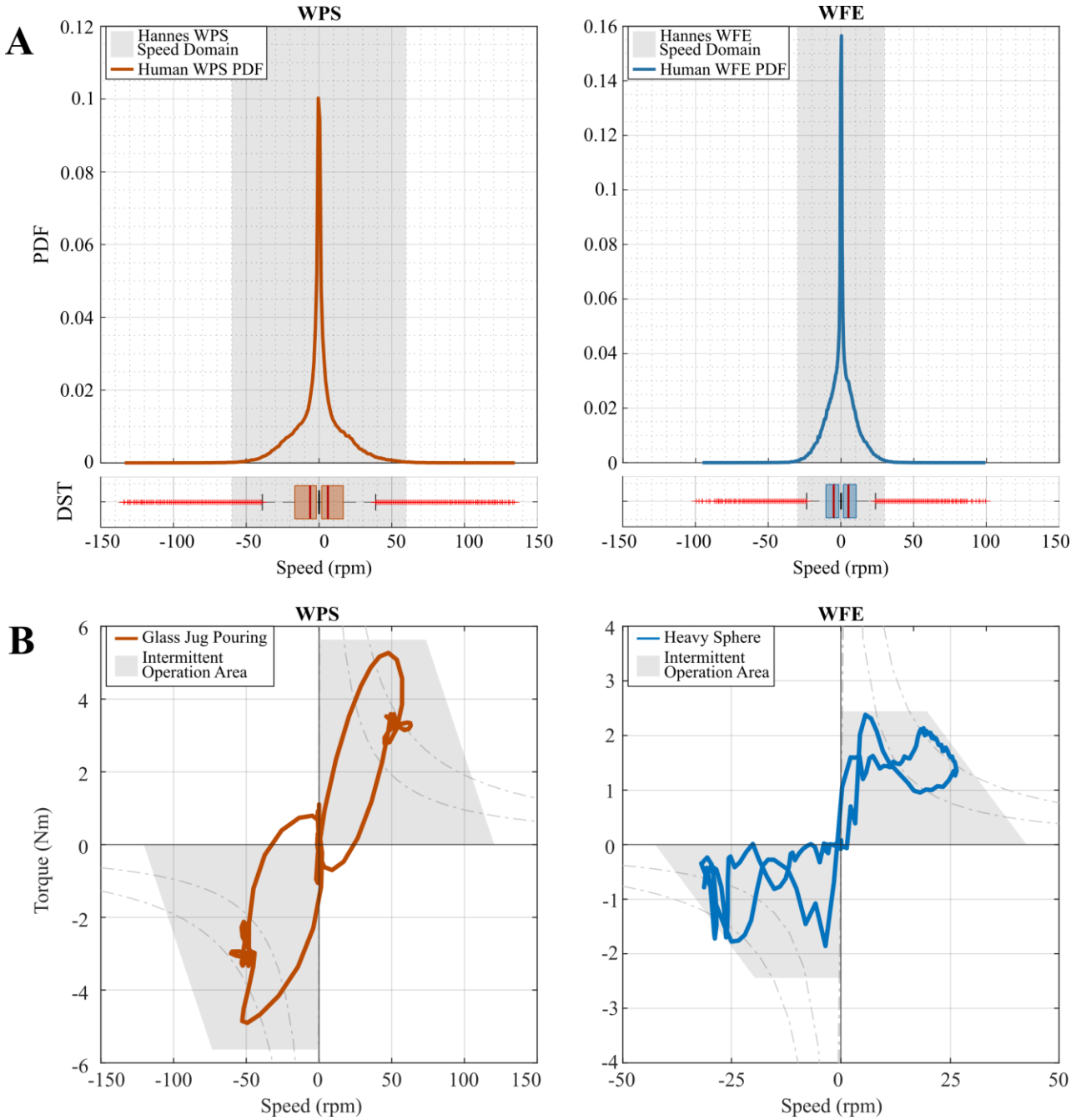

Figure 8. A) Speed Probability Density Function (PDF) and Distribution (DST) for WFE and WPS extracted from humans, the grey shaded area represents the speed's ranges of the 2-DoFs Wrist. B) Torque-Speed Behavior of WPS and WFE in 2 tasks with respect to the motor's Intermittent Operation Area.

with 6 EMG sensors (Figure 6A). The compact wrist mechatronic solution promoted anthropomorphism (Figure 6B), and joint position control was demonstrated (Figure 6C). Users could independently control joints by varying muscle contraction for speed modulation and stop movements by relaxing muscles, enhancing grasp robustness and object manipulation capabilities.

VII. Conclusion

The Hannes hand combined with the 2-DoFs wrist module is a novel prosthetic device designed to replicate human capabilities, thereby restoring lost functions for trans-radial amputees. The power trains for wrist motion allow for an impressive range of motion that is coherent with the natural equivalent, as validated by a set of functional tasks and measurement campaign. Nonetheless, anthropomorphism and mechatronic performances are guaranteed while respecting the biological requirements for weight and length as the weight exceeds of about 70g and the length exceeds about 4mm its natural counterpart (please refer to Table I and Figure 1 respectively).

Through a series of functional tasks designed to assess human wrist capabilities, we validated the performance of our prosthetic device consisting of a polyarticulated hand prosthesis and a 2-DoFs actuated wrist. Our measurement campaign provided a statistical analysis of range of motion and velocities during activities of daily living for healthy subjects. The results demonstrate that our system is capable of mimicking human movements, while also achieving a satisfactory range of motion through the use of two power trains for wrist motion. In addition, we validated the mechatronic design of the wrist through estimation of motors' torque and power effort in worst-case load and speed scenarios. Our findings demonstrate that the proposed system is a promising prosthetic device for promoting wrist dexterity for trans-radial amputees. The combination of 2-DoFs wrist

motors enables both fast and slow motions, allowing users to move freely in three-dimensional space. Moreover, the non-backdrivability of the wrist in flexion-extension provides users with the ability to hold weights or lean on the wrist for support during activities such as standing up from a chair, thus restoring not only functionality but also self-confidence in daily activities while using their prosthesis.

The results of this study suggest a potential synergy between performance and user requirements, which may indicate a promising path for designing a medical wearable device that could better address the user needs. The wrist system's design carefully mimics natural human motion while addressing anthropomorphism and low-noise requirements. This approach aimed balance performance and user needs, which could be important for achieving favorable outcomes. However, it is important to note that the study did not include real long-term use, validation of robustness, or assessments of usability satisfaction. These critical aspects will be addressed in future studies. However, these findings could still serve as a basis for future developments, providing a starting point for further refinements of the final device. Furthermore, the mechatronic system can serve as a platform for the development of novel advanced control strategies, such as the application of artificial intelligence, spanning across the invasive and non-invasive domains, bridging the gap between a state-of-the-art neuroprosthetic device and a realistic one.

Lastly, the proposed development approach can be adapted to the design of a novel trans-humeral prosthetic solution, expanding the reach of this technology to an even broader population.

ACKNOWLEDGMENT

Authors acknowledge Paolo Rossi, Paolo Bianchino and Astrid Florio for their support during the mechanical testing phase and assembly of the device. This work was supported by the Istituto Nazionale Assicurazione Infortuni sul Lavoro, under grant agreements PPR AS 1/1 and PR19-PAS-P1. The Open University Affiliated Research Centre at Istituto Italiano di Tecnologia (ARC@IIT) is part of the Open University, Milton Keynes MK7 6AA, United Kingdom.

REFERENCES

[1] A. Saradjian, A. R. Thompson, and D. Datta, "The experience of men using an upper limb prosthesis following amputation: positive coping and minimizing feeling different," *Disability and Rehabilitation*, vol. 30, no. 11, pp. 871-883, 2008.

[2] F. Mereu, F. Leone, C. Gentile, F. Cordella, E. Gruppioni, and L. Zollo, "Control Strategies and Performance Assessment of Upper-Limb TMR Prostheses: A Review," *Sensors*, vol. 21, no. 6, p. 1953, 2021.

[3] E. A. Biddiss and T. T. Chau, "Upper limb prosthesis use and abandonment: a survey of the last 25 years," *Prosthetics and orthotics international*, vol. 31, no. 3, pp. 236-257, 2007.

[4] C. Castellini, "Upper Limb Active Prosthetic systems—Overview," in *Wearable Robotics*: Elsevier, 2020, pp. 365-376.

[5] A. J. a. G. Spiers, Yuri and Dollar, Aaron M., "Examining the Impact of Wrist Mobility on Reaching Motion Compensation Across a Discretely Sampled Workspace," presented at the IEEE International Conference on Biomedical obotics and Biomechatronics (Biorob), Enshede, The Netherlands, August 26-29, 2018.

[6] G. Gillen, R. Goldberg, S. Muller, and J. Straus, "The Effect of Wrist Position on Upper Extremity Function While Wearing a Wrist Immobilizing Splint," *JPO: Journal of Prosthetics and Orthotics*, vol. 20, no. 1, pp. 19-23, 2008, doi: 10.1097/JPO.0b013e31815f013f.

[7] N. R. Olsen *et al.*, "An adaptable prosthetic wrist reduces subjective workload," *bioRxiv*, p. 808634, 2019.

[8] A. G. Mell, B. L. Childress, and R. E. Hughes, "The effect of wearing a wrist splint on shoulder kinematics during object manipulation," *Arch Phys Med Rehabil*, vol. 86, no. 8, pp. 1661-4, Aug 2005, doi: 10.1016/j.apmr.2005.02.008.

[9] T. a. F. Bertels, Kerstin and Schmalz, Thomas, "Biomechanical Analysis in Arm Prosthetics - Objectifying of Functional Advantages offered by Wrist Flexion," presented at the Myoelectric Controls/Powered Prosthetics Symposium, Fredericton, New Brunswick, Canada, August 13-15, 2008.

[10] B. Peerdeman *et al.*, "Myoelectric forearm prostheses: state of the art from a user-centered perspective," *J Rehabil Res Dev*, vol. 48, no. 6, pp. 719-37, 2011, doi: 10.1682/jrrd.2010.08.0161.

[11] L. Cappello, D. D'Accolti, M. Gherardini, M. Controzzi, and C. Cipriani, "A 2-Degree-of-Freedom Quasi-Passive Prosthetic Wrist With Two Levels of Compliance," *IEEE Robotics and Automation Letters*, vol. 8, no. 3, pp. 1231-1238, 2022.

[12] N. M. a. S. Bajaj, Adam J. and Dollar, Aaron M., "State of the Art in Prosthetic Wrists: Commercial and Research Devices," *IEEE International Conference on Rehabilitation Robotics (ICORR)*, p. 8, 2015.

[13] F. Montagnani, M. Controzzi, and C. Cipriani, "Is it Finger or Wrist Dexterity That is Missing in Current Hand Prostheses?," *IEEE Trans Neural Syst Rehabil Eng*, vol. 23, no. 4, pp. 600-9, Jul 2015, doi: 10.1109/TNSRE.2015.2398112.

[14] Ottobock. "Eletric wrist rotator." https://shop.ottobock.us/Prosthetics/Upper-Limb-Prosthetics/Myo-Hands-and-Components/Myo-Wrist-Units-and-Rotation/Electric-Wrist-Rotator/p/10S17 (accessed.

[15] Fillauer. "MC standard wrist rotator." https://fillauer.com/products/mc-standard-wrist-rotator/ (accessed.

[16] F. f. M. Control, "Powered flexion wrist." [Online]. Available: https://fillauer.com/wp-content/uploads/2020/07/MC-Powered-Flexion-Wrist-Sell-Sheet-07-28-2020.pdf.

[17] Keshen. "KS-Bionic Hand." http://en.keshen.com/product-2.html (accessed.

[18] A. Demofonti, G. Carpino, N. L. Tagliamonte, G. Baldini, L. Bramato, and L. Zollo, "Design of a modular and compliant wrist module for upper limb prosthetics," *The Anatomical Record*, vol. 306, no. 4, pp. 764-776, 2023.

[19] P. J. Kyberd, A. S. Poulton, L. Sandsjö, S. Jönsson, B. Jones, and D. Gow, "The ToMPAW Modular Prosthesis: A Platform for Research in Upper-Limb Prosthetics," *JPO: Journal of Prosthetics and Orthotics*, vol. 19, no. 1, pp. 15-21, 2007, doi: 10.1097/JPO.0b013e31802d46f8.

[20] J. H. U.-A. P. L. (APL). "Modular Prosthetic Limb (MPL) v1." https://www.jhuapl.edu/prosthetics/program (accessed.

[21] M. Bionics. "Luke Arm." https://www.mobiusbionics.com/luke-arm/ (accessed.

[22] "Atom Touch artificial arm." https://atomlimbs.com (accessed.

[23] M. Laffranchi *et al.*, "The Hannes hand prosthesis replicates the key biological properties of the human hand," *Science Robotics*, vol. 5, no. 46, 2020.

[24] D. Di Domenico *et al.*, "Hannes Prosthesis Control Based on Regression Machine Learning Algorithms," presented at the 2021 IEEE/RSJ International Conference on Intelligent Robots and Systems (IROS 2021), 2021.

[25] A. Marinelli *et al.*, "Performance Evaluation of Pattern Recognition Algorithms for Upper Limb Prosthetic Applications," in *8th IEEE RAS/EMBS International Conference for Biomedical Robotics and Biomechatronics (BioRob)*, 2020: IEEE.

[26] K. Nazarpour, "A more human prosthetic hand," *Science Robotics*, vol. 5, no. 46, p. eabd9341, 2020, doi: 10.1126/scirobotics.abd9341.

[27] I. A. Kapandji, Monduzzi, Ed. *Fisiologia articolare, vol. 1, Arto Superiore*, 6 ed. 2011.

[28] D. A. Neumann, *Kinesiology of the Muscoloskeletal System* (Foundations for Physical Rehabilitation). Mosby.

[29] R. Tubiana, J.-M. Thomine, and E. Mackin, *Examination of the Hand and Wrist*. Taylor & Francis Group, 1998.

[30] E. Biddiss and T. Chau, "Upper-limb prosthetics: critical factors in device abandonment," *Am J Phys Med Rehabil*, vol. 86, no. 12, pp. 977-87, Dec 2007, doi: 10.1097/PHM.0b013e3181587f6c.

[31] C. Cipriani, R. Sassu, M. Controzzi, and M. C. Carrozza, "Influence of the weight actions of the hand prosthesis on the performance of pattern recognition based myoelectric control: Preliminary study," 2011.

[32] ISHN. "https://www.ishn.com/articles/97844-statistics-on-hand-and-arm-loss." (accessed.

[33] NASA. "https://msis.jsc.nasa.gov/sections/section03.htm." (accessed.

[34] A. Marinelli *et al.*, "Active upper limb prostheses: A review on current state and upcoming breakthroughs," *Progress in Biomedical Engineering*, 2022.

[35] J. C. Perry, J. Rosen, and S. Burns, "Upper-limb powered exoskeleton design," *IEEE/ASME transactions on mechatronics*, vol. 12, no. 4, pp. 408-417, 2007.

[36] C. M. Light, P. H. Chappell, and P. J. Kyberd, "Establishing a standardized clinical assessment tool of pathologic and prosthetic hand function: normative data, reliability, and validity," *Archives of physical medicine and rehabilitation*, vol. 83, no. 6, pp. 776-783, 2002.

[37] S. A. F. Taylor, A. E. Kedgley, A. Humphries, and A. F. Shaheen, "Simulated activities of daily living do not replicate functional upper limb movement or reduce movement variability," *Journal of Biomechanics*, vol. 76, pp. 119-128, 2018, doi: https://doi.org/10.1016/j.jbiomech.2018.05.040.

[38] H. Burger, F. Franchignoni, A. W. Heinemann, S. Kotnik, and A. Giordano, "Validation of the orthotics and prosthetics user survey upper extremity functional status module in people with unilateral upper limb amputation," *Journal of rehabilitation medicine*, vol. 40, no. 5, pp. 393-399, 2008.

[39] P. J. Kyberd *et al.*, "Two-degree-of-freedom powered prosthetic wrist," *J Rehabil Res Dev*, vol. 48, no. 6, pp. 609-17, 2011, doi: 10.1682/jrrd.2010.07.0137.

[40] D. A. Bennett, J. E. Mitchell, D. Truex, and M. Goldfarb, "Design of a Myoelectric Transhumeral Prosthesis," *IEEE/ASME Transactions on Mechatronics*, vol. 21, no. 4, pp. 1868-1879, 2016, doi: 10.1109/TMECH.2016.2552999.

[41] N. M. Bajaj, A. J. Spiers, and A. M. Dollar, "State of the art in artificial wrists: A review of prosthetic and robotic wrist design," *IEEE Transactions on Robotics*, vol. 35, no. 1, pp. 261-277, 2019.

[42] Southampton. "Southampton Hand Assessment Procedure (SHAP) " http://www.shap.ecs.soton.ac.uk/index.php (accessed.

[43] R. Safaee-Rad, E. Shwedyk, A. O. Quanbury, and J. E. Cooper, "Normal functional range of motion of upper limb joints during performance of three feeding activities," (in eng), *Arch Phys Med Rehabil*, vol. 71, no. 7, pp. 505-9, Jun 1990.

[44] D. H. Gates, L. S. Walters, J. C. Cowley, J. M. Wilken, and L. J. Resnik, "Range of Motion Requirements for Upper-Limb Activities of Daily Living," *The American journal of occupational therapy : official publication of the American Occupational Therapy Association*, vol. 70 1, pp. 7001350010p1-7001350010p10, 2016.

[45] A. Naceri *et al.*, "From human to robot grasping: force and kinematic synergies: Close comparison between human and robotic hands in both force and kinematic domain," in *Tactile Sensing, Skill Learning, and Robotic Dexterous Manipulation*: Elsevier, 2022, pp. 133-148.

[46] M. Luchetti, A. G. Cutti, G. Verni, R. Sacchetti, and N. Rossi, "Impact of Michelangelo prosthetic hand: Findings from a crossover longitudinal study," *Journal of rehabilitation research and development*, vol. 52, 5, p. 13, 2015, doi: http://dx.doi.org/10.1682/JRRD.2014.11.0283.

[47] M. Semprini *et al.*, "Clinical evaluation of Hannes: measuring the usability of a novel polyarticulated prosthetic hand," in *Tactile Sensing, Skill Learning, and Robotic Dexterous Manipulation*: Elsevier, 2022, pp. 205-225.

[48] J. R. Binda, "Multiple degrees of freedom wrist prostheses," Master of Science, Biorobotics, Delft University of Technology, 2018.
[49] Ottobock. "Ottobock Hand Chassis." https://shop.ottobock.us/c/Hand-Chassis-with-Quick-Disconnect-Wrist/p/9S266 (accessed.
[50] Ottobock. "Coaxial Plug." https://shop.ottobock.us/Prosthetics/Upper-Limb-Prosthetics/bebionic/Myoelectric-Accessories/Coaxial-Plug/p/9E169 (accessed.
[51] Ottobock. "Co-Axial Bushing." https://shop.ottobock.us/c/Co-Axial-Bushing/p/9E397 (accessed.
[52] D. Shah, Y. Wu, A. Scalzo, G. Metta, and A. Parmiggiani, "A Comparison of Robot Wrist Implementations for the iCub Humanoid †," *Robotics*, vol. 8, no. 1, p. 11, 2019. [Online]. Available: https://www.mdpi.com/2218-6581/8/1/11.
[53] R. Damerla *et al.*, "Design and Testing of a Novel, High-Performance Two DoF Prosthetic Wrist," *IEEE Transactions on Medical Robotics and Bionics*, 2022.
[54] Ottobock. "Hand Chassis with Quick Disconnect Wrist." https://shop.ottobock.us/c/Hand-Chassis-with-Quick-Disconnect-Wrist/p/9S266 (accessed.
[55] TQ. "TQ ILM25x04 Datasheet." https://www.tq-group.com/filedownloads/files/products/robodrive/data-sheets/en/DRVA_DB_Servo-Kits_ILM_EN_Rev408_Web.pdf (accessed.
[56] Ottobock. "Lamination Ring." https://shop.ottobock.us/Prosthetics/Upper-Limb-Prosthetics/Myo-Hands-and-Components/Myo-Wrist-Units-and-Rotation/Lamination-Ring/p/10S1 (accessed.
[57] Ottobock. "Electric Wrist Rotator." https://shop.ottobock.us/Prosthetics/Upper-Limb-Prosthetics/Myo-Hands-and-Components/Myo-Wrist-Units-and-Rotation/Electric-Wrist-Rotator/p/10S17 (accessed.
[58] T. Instruments. "Microcontroller." https://www.ti.com/lit/ds/symlink/tm4c123gh6pm.pdf (accessed.
[59] B. Sensortech. "BNO055 Datasheet." https://www.bosch-sensortec.com/media/boschsensortec/downloads/datasheets/bst-bno055-ds000.pdf (accessed.
[60] AMS. "Magnetic Encoder." https://ams.com/documents/20143/36005/AS5045B_DS000397_2-00.pdf (accessed.
[61] A. Marinelli *et al.*, "Miniature EMG Sensors for Prosthetic Applications," 2021.
[62] S. A. Taylor, A. E. Kedgley, A. Humphries, and A. F. Shaheen, "Simulated activities of daily living do not replicate functional upper limb movement or reduce movement variability," *Journal of Biomechanics*, vol. 76, pp. 119-128, 2018.
[63] R. Khusainov, D. Azzi, I. E. Achumba, and S. D. Bersch, "Real-time human ambulation, activity, and physiological monitoring: Taxonomy of issues, techniques, applications, challenges and limitations," *Sensors*, vol. 13, no. 10, pp. 12852-12902, 2013.
[64] E. Scheme and K. Englehart, "Electromyogram pattern recognition for control of powered upper-limb prostheses: state of the art and challenges for clinical use," *Journal of Rehabilitation Research & Development*, vol. 48, no. 6, 2011.
[65] H. Hermens, S. Stramigioli, H. Rietman, P. Veltink, and S. Misra, "Myoelectric forearm prostheses: State of the art from a user-centered perspective," *J. Rehabil. Res. Dev.*, vol. 48, no. 6, p. 719, 2011.

Nicolò Boccardo (IEEE Member) holds a B.Sc. degree in Biomedical Engineering and an M.Sc. degree in Robotics Engineering from the University of Genoa (Italy), earned in 2011 and 2013, respectively. He has a diverse range of professional experience, having worked as a fellow researcher at the European Centre of Nuclear Research (CERN) in Geneva (Switzerland), focusing on high-precision particle beam collimation, and in the transportation industry at Bombardier. In 2014, he joined the Italian Institute of Technology (IIT), where he was involved in the development of the Hannes prosthetic system and has since been actively engaged in technology transfer and product development activities. Currently, he serves as the Chief Mechatronic Engineer and Team Leader of the Hannes prosthetic system project at the Rehab Technologies Laboratory (IIT) in Genoa (Italy), where he leverages his extensive expertise in hi-tech medical devices to develop novel mechatronic systems in the robotics and prosthetics field.

Michele Canepa (IEEE Member) received the B.Sc degree and the M.Sc degree in Electrical Engineering at the University of Genoa in 2010 and 2014 respectively. He worked as a fellow researcher at University of Genoa, focusing on developing embedded electrical measurements instruments. In 2014 joined Italian Institute of Technology to develop electrical and electronic systems for robotic medical devices. Since then, he designed electronics for upper and lower limb prostheses, lower limb exoskeletons and rehabilitation robots. In 2017 joined the IIT startup company Movendo Technology as Lead Electrical Engineer. Currently he is Senior Electrical Engineer and Team Leader of the Electronics Team at the Rehab Technologies Laboratory (IIT) in Genoa (Italy). His expertise lies in the development and industrialization of electrical systems for robotic medical devices.

Samuel Stedman received his MEng degree in Mechanical Engineering and German at the University of Sheffield in 2015. He worked as a Mechanical Engineer for the INAIL Rehab Lab at the Istituto Italiano di Tecnologia (IIT) between 2018 and 2022, primarily on the mechanical design of upper limb prosthetics. Currently he is a Senior Robotics Research Engineer at the Dyson Robotics Centre, UK. His expertise lies in the product development of medical devices and consumer robotics, as well as the

mechatronic design of high-performance robotic actuators for upper limb prosthetics and robot manipulation.

Lorenzo Lombardi joined Imperial College of London where he obtained his M.Eng. in Biomedical Engineering with Electronics in 2016. In 2017, he joined the Rehabilitation Technology laboratory at the Italian Institute of Technology as an Electronics Engineer. Here he was responsible for the development of the electronics and firmware of a prosthetic upper-limb system. The application focused on sensors (EMGs and IMUs), battery management and motor control. He is now pursuing a Ph.D. in Biomedical Engineering at Washington University in St. Louis under the supervision of Dr. Ismael Seanez on brain computer interfaces for spinal cord injury. His interests include medical robotics and biological signal processing.

Andrea Marinelli, (Student Member, IEEE), received the B.Sc. degree in Biomedical Engineering from Università Politecnica delle Marche, Ancona, Italy, in 2016 and the M.Sc. degree in bioengineering and neuroengineering from the Faculty of Engineering University of Genova, Genova, Italy, in 2019. He is currently pursuing the Ph.D. degree in Bioengineering and Robotics at University of Genova. From 2019, he is collaborating with the Rehab Technologies Lab at Italian institute of Technologies, Genova, Italy. His research interest includes the development of Body Machine Body Interfaces for upper limb amputees using electromyographic signals and machine learning algorithms to decode and reproduce intended movements. He is also the software engineer of Hannes prosthetic system developed by Italian Institute of Technology (IIT) and Istituto Nazionale per l'Assicurazione contro gli Infortuni sul Lavoro (INAIL) to realize a fully actuated upper limb prosthesis.

Dario Di Domenico, (Student Member, IEEE), received a B.Sc. in biomedical engineering and a M.Sc. in mechatronic engineering from Politecnico di Torino (Italy) in 2018 and 2020, respectively. He was then hired for a year as Research Fellow in the Rehab Technologies Lab of Istituto Italiano di Tecnologia (IIT - Genova, Italy). He is currently Ph.D. candidate in Electrical, Electronics and Communications Engineering at IIT and Politecnico di Torino. His research interests include biological signal processing, adaptive control algorithms and pattern recognition methods for advanced myoelectric control of prosthetic systems.

Riccardo Galviati received a B.Sc. in medical engineering from University of Rome Tor Vergata in 2019 and a M.Sc. in biomedical engineering from Politecnico di Milano in 2022. He was then hired as Software Engineer for the Hannes team in the Rehab Technologies Lab of Istituto Italiano di Tecnologia (IIT - Genova, Italy). His expertise lies in the development of novel control strategies for robotic medical devices.

Emanuele Gruppioni (IEEE Member) received his Master's Degree in Electronic Engineering with Biomedical specialization in 2006, issued by the University of Bologna. Since 2006 he works as researcher at Centro Protesi Inail, the main prosthetic centre in Italy. In 2014 he received the university degree of C.P.O. (Certified Prosthetist and Orthotist) and in 2020 the Ph.D. in Bioengineering and Bioscience issued by the University Campus BioMedico of Rome. Since 2015 he is professor of the course of "Orthoses and Orthopaedic Aids III", faculty of medicine and surgery, University of Bologna. Currently he is the Technical Director of the Research and Training Area at Centro Protesi Inail, where is the manager of several projects in collaboration with important research institutions. His activities mainly concern prosthetic limbs and new medical devices for rehabilitation, from its design and development to the clinical studies for certification.

Lorenzo De Michieli, (Member, IEEE), is Director of the Rehab Technologies Lab at the Italian Institute of Technology (IIT), an Innovation Lab aimed to develop new prostheses, exoskeletons and rehabilitation devices of high market potential in the healthcare sector. He received a M.S. in Physics (Material Science) in 1999, and a Ph.D. in Mechanical Engineering (Humanoid Robotics) from the University of Genoa, Italy. He also accomplished an extensive training on innovation management both in Italy at Jacobacci & Partners (Turin, IT) and abroad at the European Patent Office (The Hague, NL) and the Bergen Teknologioverføring (Bergen, N). From 2014 to 2019 he was contract Professor at the University of Genoa - Faculty of Economics - in Collaborative Innovation and Technology Transfer. Before joining IIT in 2008, he was research technologist at the National Institute for the Physics of Matter (INFM, Italy) from 2002 to 2006, and at the National Research Council (CNR, Italy) from 2006 to 2008, gaining an extensive experience in developing industrial alliances and managing competitive industrial R&D projects.

Matteo Laffranchi, (IEEE Member), Matteo Laffranchi received his Master's Degree in Mechatronics Engineering at Polytechnic of Turin in 2006 and a PhD in Robotics from the University of Sheffield in 2011. After a brief experience in the automation industry at OSAI A.S., from 2008 to 2011 he was a research fellow at the Italian Institute of Technology (IIT) and a postdoctoral researcher at the same institute from 2011 to 2014. Since then, he is actively involved into technology transfer and product development activities. During his PhD and Post-Doc, he spent 6 years developing compliant actuators and robots for safe human robot collaboration. Currently, he is Coordinator of Robotics at the Rehab Technologies Lab (IIT), with focus on the development of healthcare wearable robots.